Vector-vortex Bessel–Gauss beams and their tightly focusing properties

Kun Huang,[1,2] Peng Shi,[2] G. W. Cao,[2] Ke Li,[2] X. B. Zhang,[3] and Y. P. Li[1,2,*]

[1]*Key Laboratory of Quantum Information, China Academy of Science, Hefei, Anhui 230026, China*

[2]*Department of Optics and Optical Engineering, University of Science and Technology of China, Hefei, Anhui 230026, China*

[3]*National Synchrotron Radiation Laboratory, University of Science and Technology of China, Hefei, Anhui 230026, China*

**Corresponding author: liyp@ustc.edu.cn*

Received September 27, 2010; revised December 19, 2010; accepted February 1, 2011;
posted February 11, 2011 (Doc. ID 135704); published March 9, 2011

We demonstrate that the amplitude of vector-vortex beams has a Bessel–Gauss (BG) distribution through a rigorous vector electromagnetic analysis. We also investigate the intensity profiles in the focal plane of vector-vortex beams that are focused by a high numerical-aperture lens obeying the Helmholtz condition. Although the intensity of a vector-vortex BG beam with a topological charge $n = 1$ is nonzero along the axis in the focal plane, the beams with $n \neq 1$ show discrete multiple spots which can be useful for optical trapping.

OCIS codes: 260.5430, 260.6042, 180.0180, 170.4520.

During the past few years, much attention has been paid to beams with a vector-vortex polarization profile, which has a polarization that depends linearly on the polar angle. For a vector-vortex beam traveling in the z axis, the vector amplitude of the electric field is expressed as $\mathbf{F}(r,\varphi,z) = A \cdot [\cos(n\varphi+\varphi_0)\mathbf{e}_x + \sin(n\varphi+\varphi_0)\mathbf{e}_y]$, where r and φ are the polar coordinates, A is the module of the vector amplitude, n is an integer, φ_0 represents the direction of the vector where $\varphi = 0$, and $\mathbf{e}_x$ and $\mathbf{e}_y$ are the unit vectors. Experimentally, some methods have been introduced to generate the vector-vortex beams, such as, space-variant subwavelength gratings [1], using a twisted nematic liquid-crystal device [2], and the interference of two circular-polarization Laguerre–Gauss (LG) beams with opposite helical index [3,4]. The intensity profiles of vector-vortex beams that have been reported have no dependence on the angle, which means that module A is also independent on the φ coordinate. Theoretically, few people have investigated the amplitude of the vector-vortex beams. Using the superposition of two circular-polarization LG beams, Maurer *et al.* have demonstrated that the vector-vortex beams have the amplitude with an LG distribution [3]. Through the rigorous vector electromagnetic analysis, we find that the vector-vortex beams have the amplitude with a Besse–Gauss (BG) profile. In addition, the vector-vortex BG beam is one of the vector solutions of Helmholtz equation in the paraxial approximation.

Interestingly, the vector-vortex beam with $n = 1$ and $\varphi_0 = 0$ is the well-known radially polarized beam [5], which has been applied in microscopy, optical trapping, optical storage, single molecule orientation imaging, and nanofocusing. Recently, the vector-vortex beams have been used to realize the remote preparation of two-qubit hybrid entangled states for quantum communication [6]. Nevertheless, vector-vortex beams usually exhibit their advantages in tight focusing systems. For example, when focused by a high numerical-aperture (NA) lens, a radially polarized beam ($n = 1$) can give an extremely sharp focus [7] or a spot with subdiffraction size [8,9] in the focal plane. Therefore, the tightly focusing properties of vector-vortex BG beams ($|n| > 1$) have been investigated in this Letter. For the focused vector-vortex BG beams ($n > 2$ and $n < 0$), the spots in the focal plane have the null intensity on the optical axis and the angle-variant intensity, which can be used in optical tweezers with multitraps [10].

For a vector beam traveling in the z axis, the electric field $\mathbf{E}$ can be described by the vector Helmholtz equation:

$$\nabla \times \nabla \times \mathbf{E} - k^2\mathbf{E} = 0, \tag{1}$$

where $k = \omega/c$, ω is the frequency, and c is the light speed in vacuum. In polar coordinates, the electric field $\mathbf{E}$ with a vector amplitude $\mathbf{F}$ is

$$\mathbf{E}(r,\varphi,z,t) = \mathbf{F}(r,\varphi,z)\exp[i(kz-\omega t)], \tag{2}$$

where the vector amplitude $\mathbf{F} = F_r\mathbf{e}_r + F_\varphi\mathbf{e}_\varphi$ is transverse, having only the $\mathbf{e}_r$ and $\mathbf{e}_\varphi$ components. Taking account of the paraxial ($\partial^2\mathbf{F}/\partial z^2 \approx 0$) and slowly varying envelope approximations ($\partial\mathbf{F}/\partial z \ll k\mathbf{F}$), one can substitute Eq. (2) in Eq. (1), producing two coupled partial differential equations about the components of the vector amplitude $\mathbf{F}$:

$$\frac{1}{r}\frac{\partial}{\partial r}\left(r\frac{\partial F_r}{\partial r}\right) - \frac{1}{r^2}F_r - \frac{2}{r^2}\frac{\partial F_\varphi}{\partial \varphi} + \frac{1}{r^2}\frac{\partial^2 F_r}{\partial \varphi^2} + 2ik\frac{\partial F_r}{\partial z} = 0, \tag{3}$$

$$\frac{1}{r}\frac{\partial}{\partial r}\left(r\frac{\partial F_\varphi}{\partial r}\right) - \frac{1}{r^2}F_\varphi + \frac{2}{r^2}\frac{\partial F_r}{\partial \varphi} + \frac{1}{r^2}\frac{\partial^2 F_\varphi}{\partial \varphi^2} + 2ik\frac{\partial F_\varphi}{\partial z} = 0. \tag{4}$$

Equations (3) and (4) are valid for an arbitrary vector beam in the paraxial approximation in polar coordinates. Concerning the vector-vortex beams discussed here, the vector amplitude $\mathbf{F}$ in the polar coordinate is expressed as $\mathbf{F}(r,\varphi,z) = A(r,z)\{\cos[(n-1)\varphi+\varphi_0]\mathbf{e}_r + \sin[(n-1)\varphi+\varphi_0]\mathbf{e}_\varphi\}$, where $F_r = A(r,z)\cos[(n-1)\varphi+\varphi_0]$ and $F_\varphi = A(r,z)\sin[(n-1)\varphi+\varphi_0]$. After inserting the components F_r and F_φ of the vector-vortex beams, Eqs. (3) and (4) are simplified to the same equation:

$$\frac{1}{r}\frac{\partial}{\partial r}\left(r\frac{\partial A}{\partial r}\right)-\frac{n^2}{r^2}A+2ik\frac{\partial A}{\partial z}=0, \tag{5}$$

which is a linear homogenous partial differential equation. By direct substitution, one can show that Eq. (5) has the exact solution:

$$A(r,z)=\frac{1}{1+iz/z_0}\exp\left(-\frac{r^2/w_0^2}{1+iz/z_0}\right)\cdot\exp\left[-\frac{i\beta^2 z/(2k)}{1+iz/z_0}\right]J_n\left(\frac{\beta r}{1+iz/z_0}\right), \tag{6}$$

where J_n is the n-order Bessel function of the first kind, and β is a constant that determines the beam profile. When $\beta=0$ and $n=0$, $A(r,z)$ is the scalar solution of the elementary Gaussian beam, whose waist radius is w_0 and Rayleigh range is z_0. The vector-vortex beams have the positive β in this Letter. Figure 1 displays the intensity profiles and vector plots of the vector-vortex BG beams with $n=-1$, 1, 2, and 3 in the waist plane. As depicted in Fig. 1, the polarization of the beam varies uniformly while the intensity is angle independent. Because of the uncertain polarization (vector singularity) at the center, the vector-vortex BG beams have null on-axis intensity. Affected by the vector singularity, vector-vortex BG beams have low intensity in the tiny area around the beam center. As $|n|$ increases, the uncertainty of polarization increases around the beam center, enlarging the low-intensity area, which was observed experimentally [4]. In Fig. 1, in order to obtain the single-ring-shaped vector-vortex BG beam, we choose the beam parameters $w_0=2.5\,\mathrm{mm}$ and $\beta=0.5\,\mathrm{mm}^{-1}$. By changing w_0 and β, one can achieve the multiring-shaped beams, which were realized experimentally [11] and could be used to reduce the spot size [12] in the focal plane for a focused radially polarized beam ($n=1$). For simplicity, we assume that the vector-vortex BG beams mentioned in the following have the single–ring–shaped intensity.

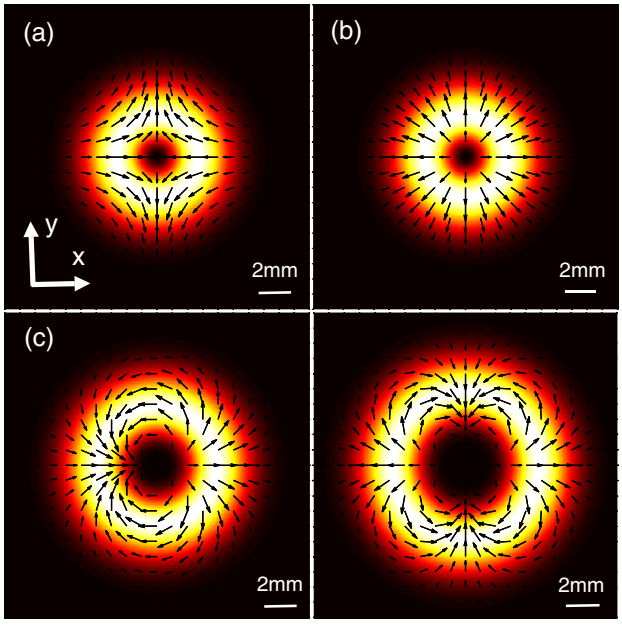

Fig. 1. (Color online) Intensity and vector plots of the vector-vortex BG beams with $n=-1$, 1, 2, 3 and $\varphi_0=0$ in the waist plane. The beam parameters are $w_0=2.5\,\mathrm{mm}$ and $\beta=0.5\,\mathrm{mm}^{-1}$. (a) $n=-1$; (b) $n=1$, the radially polarized beam; (c) $n=2$; (d) $n=3$.

In general, the tight focusing of a vector beam is approximated by the theory of Richards and Wolf. Assuming that the vector-vortex BG beam is focused by a high NA lens obeying the Helmholtz condition [5], and the beam waist is in the pupil plane of the lens (Fig. 2), the vector electric fields in the focal region can be expressed as

$$E_\rho(\rho,\phi,z)=C\cdot i^{n+1}\cos[(n-1)\phi+\varphi_0]\int_0^\alpha P(\theta)A(\theta)[\cos\theta(J_n-J_{n-2})+(J_n+J_{n-2})]\sin\theta\cdot e^{ikz\cos\theta}d\theta, \tag{7}$$

$$E_\phi(\rho,\phi,z)=C\cdot i^{n+1}\sin[(n-1)\phi+\varphi_0]\int_0^\alpha P(\theta)A(\theta)[\cos\theta(J_n+J_{n-2})+(J_n-J_{n-2})]\sin\theta\cdot e^{ikz\cos\theta}d\theta, \tag{8}$$

$$E_z(\rho,\phi,z)=-2C\cdot i^{n}\cos[(n-1)\phi+\varphi_0]\int_0^\alpha P(\theta)A(\theta)J_{n-1}\cdot\sin^2\theta\cdot e^{ikz\cos\theta}d\theta, \tag{9}$$

where C is a constant, $\alpha=\arcsin(\mathrm{NA})$ in vacuum, $J_m=J_m(k_\rho\sin\theta)$, $P(\theta)$ is the pupil function of the beam. and $A(\theta)$ is the apodization factor of a focusing lens. For a lens obeying the Helmholtz condition, $A(\theta)=(\cos\theta)^{-3/2}$ and the pupil function of a vector-vortex BG beam is given by

$$P(\theta)=\exp\left(-\gamma^2\frac{\tan^2\theta}{\tan^2\alpha}\right)J_n\left(\beta w_0\gamma\frac{\tan\theta}{\tan\alpha}\right), \tag{10}$$

where γ, taken as unity in this Letter, is the ratio of the pupil radius and the beam waist.

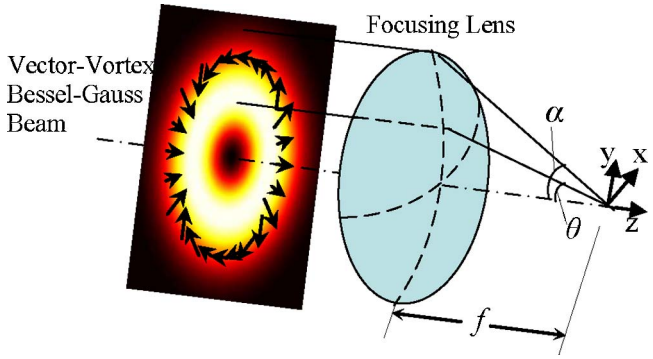

Fig. 2. (Color online) Schematic of the vector-vortex BG beams focused by a high NA lens. The origin of the coordinate system is located in the geometric focus of the lens. The waist plane of beams and the pupil plane of the lens share the same position. θ denotes the angle between the convergent ray and the optical axis.

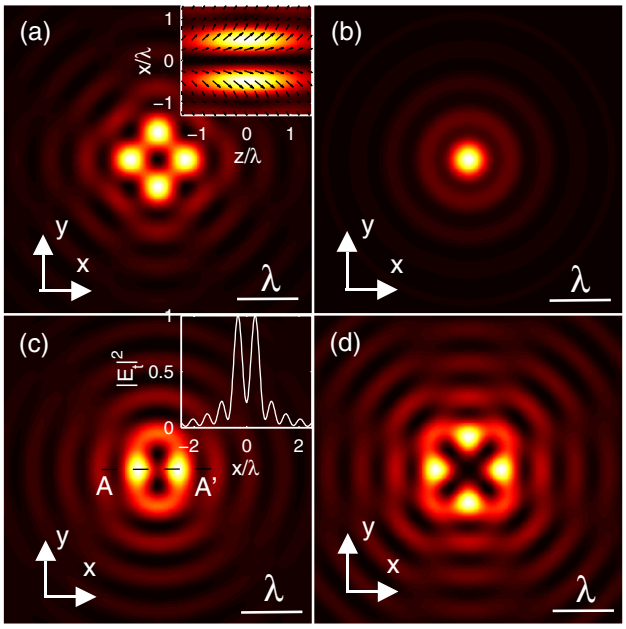

Fig. 3. (Color online) Total electric field ($|E_t|^2 = |E_\rho|^2 + |E_\phi|^2 + |E_z|^2$) in the focal plane of the focused vector-vortex BG beams with $n = -1, 1, 2, 3$ and $\varphi_0 = 0$. The NA of the focusing lens is 0.95 in vacuum. (a) $n = -1$. Inset, total electric field and polarization profile of the focused beam with $n = -1$ in the $x = z$ plane. (b) $n = 1$, the radially polarized beam. (c) $n = 2$. Inset, normalized intensity along the dashed line AA', which indicates the on-axis intensity of the focused beam with $n = 2$ is nonzero. (d) $n = 3$.

For the focused vector-vortex BG beams with the parameters $w_0 = 2.5\,\mathrm{mm}$ and $\beta = 0.5\,\mathrm{mm}^{-1}$, the numerical solutions of electric field in the focal plane are displayed in Fig. 3. The intensity of the focused radially polarized beam is angle independent [Fig. 3(b)] in the focal plane because the three electric field components, Eqs. (7)–(9), are independent on the azimuthal coordinate. When $n \neq 1$, the intensity depends on the azimuthal coordinate and the discrete main spots are obtained in the focal plane [Figs. 3(a), 3(c), and 3(d)]. The number of main spots is $2(n-1)$ for $n > 1$ and $2(|n|+1)$ for $n < 0$. The main spots in the focal plane are dominated by the radial and longitudinal components, which are both proportional to $\cos[(n-1)\phi + \varphi_0]$. The azimuthal component is located in the area between two adjacent spots. It is worthy to note that φ_0 is taken as zero in Fig. 3. When φ_0 is time dependent, which can be easily realized by using two cascaded $\lambda/2$ plates or the nonmechanical polarization-rotation device [5], the main spots rotate azimuthally. The rotated spots are relevant for optical trapping [13].

The radially polarized beam is well known for its capacity of supplying a strong longitudinal field component and on-axis intensity in the focal plane. However, for vector-vortex BG beams, the radially polarized beam is not the only one that has the on-axis intensity. The vector-vortex BG beams with $n = 1$ and $0 < \varphi_0 < \pi/2$ also have the on-axis intensity, which is lower than that of the radially polarized beam. In addition, when $n = 2$, the integrands of the radial and azimuthal components, Eqs. (7) and (8), contain the zero-order Bessel function of the first kind. Therefore, the on-axis intensity of the focused vector-vortex beam with $n = 2$ is not zero. Nevertheless, as shown in Fig. 3(c), the on-axis intensity is so low, about 1/5 of the peak intensity of the main spots, that it can be neglected. For other vector-vortex BG beams with $n \neq 1$ or 2, the on-axis intensity in the focal plane is null.

In conclusion, we have presented that the vector-vortex BG beam is one of the vector-beam solutions of Maxwell's wave equations in the paraxial approximation. The tightly focusing properties of the vector-vortex BG beams have been investigated. The focused vector-vortex BG beams with $n \neq 1$ have the azimuthally variant intensity in the focal plane. The discrete main spots can be used as the optical tweezers with multitraps, which are different from those obtained by the traditional phase modulation.

References

1. A. Niv, G. Biener, V. Kleiner, and E. Hasman, Opt. Express **14**, 4208 (2006).
2. M. Stalder and M. Schadt, Opt. Lett. **21**, 1948 (1996).
3. C. Maurer, A. Jesacher, S. Furhapter, S. Bernet, and M. Ritsch-Marte, New J. Phys. **9**, 78 (2007).
4. X. L. Wang, J. P. Ding, W. J. Ni, C. S. Guo, and H. T. Wang, Opt. Lett. **32**, 3549 (2007).
5. Q. Zhan, Adv. Opt. Photon. **1**, 1 (2009).
6. J. T. Barreiro, T. C. Wei, and P. G. Kwiat, Phys. Rev. Lett. **105**, 030407 (2010).
7. R. Dorn, S. Quabis, and G. Leuchs, Phys. Rev. Lett. **91**, 233901 (2003).
8. H. Wang, L. Shi, B. Lukyanchuk, C. Sheppard, and C. T. Chong, Nat. Photon. **2**, 501 (2008).
9. K. Huang, P. Shi, X. L. Kang, X. B. Zhang, and Y. P. Li, Opt. Lett. **35**, 965 (2010).
10. M. MacDonald, L. Paterson, K. Volke-Sepulveda, J. Arlt, W. Sibbett, and K. Dholakia, Science **296**, 1101 (2002).
11. A. Niv, G. Biener, V. Kleiner, and E. Hasman, Opt. Lett. **29**, 238 (2004).
12. Y. Kozawa and S. Sato, J. Opt. Soc. Am. A **24**, 1793 (2007).
13. S. Franke-Arnold, J. Leach, M. J. Padgett, V. E. Lembessis, D. Ellinas, A. J. Wright, J. M. Girkin, P. Ohberg, and A. S. Arnold, Opt. Express **15**, 8619 (2007).